



Shape Memory Effects Using Magnetoactive Boron–Organo–Silicon Oxide Polymers

Nina Prem, Dirk Sindesberger, Birgit Striegl, Valter Böhm, and Gareth J. Monkman*

Thermomechanical shape memory materials have certain disadvantages when it comes to 3D volumetric reproduction intended for rapid prototyping or robotic prehension. The need to constantly supply energy to counteract elastic retraction forces in order to maintain the required geometry, together with the inability to achieve conformal stability at elevated temperatures, limits the application of thermal shape memory polymers. Form removal also presents problems as most viscoelastic materials do not ensure demolding stability. This work demonstrates how magnetoactive boron–organo–silicon oxide polymers under the influence of an applied magnetic field can be used to achieve energy free sustainable volumetric shape memory effects over extended periods. The rheopectic properties of boron–organo–silicon oxide materials sustain form removal without mold distortion.

1. Introduction

Shape memory alloys (SMAs) rely on forced plastic deformation while in the martensitic (cold) state. On heating, the austenitic (warm) state is reached which allows the alloy to return (spring back) to its original shape. Despite the plastic to elastic transformation, a significant increase in Young's modulus is observed in the austenitic state. The metallic phenomenon was originally studied by Adolf Martens toward the end of the last century^[1] and the martensitic transformation responsible for metallic shape memory effect still bears his name.^[2] Shape memory polymers (SMPs) on the other hand, rely on one or more glass transition temperatures to effect a change in state.

N. Prem, D. Sindesberger, Prof. G. J. Monkman
Mechatronics Research Unit
Ostbayerische Technische Hochschule Regensburg
Regensburg 93053, Germany
E-mail: gareth.monkman@oth-regensburg.de

Dr. B. Striegl
Centre for Biomedical Engineering
Ostbayerische Technische Hochschule Regensburg
Regensburg 93053, Germany
Prof. V. Böhm
Fakultät Maschinenbau
Ostbayerische Technische Hochschule Regensburg
Regensburg 93053, Germany

The ORCID identification number(s) for the author(s) of this article can be found under <https://doi.org/10.1002/macp.202000149>.

© 2020 The Authors. Published by WILEY-VCH Verlag GmbH & Co. KGaA, Weinheim. This is an open access article under the terms of the Creative Commons Attribution License, which permits use, distribution and reproduction in any medium, provided the original work is properly cited.

DOI: 10.1002/macp.202000149

Contrary to their metallic counterparts, SMPs exhibit a reduction in Young's modulus with increasing temperature. For an excellent comparison of SMAs and polymers, readers should consult.^[3]

Whether metal alloys^[4] or polymers,^[5] the field of shape memory effect has been hitherto dominated by thermomechanical effects^[6,7] which inevitably demand a continuous flow of energy to compensate for thermal losses. Using SMA, conformable volumes are difficult to realize. By using SMPs, particularly in foam form, 3D shape memory is possible.^[8] For structural strengthening purposes, the inclusion of carbon fiber^[9] and similar structural materials is common. The number of poly-

meric shape memory effects is vast and for a full coverage of the topic there exists extensive review literature.^[7,10,11]

Magnetoactive polymers are elastomeric composites comprising a nonmagnetic polymer matrix and a distribution of magnetically susceptible micrometer sized ferromagnetic or paramagnetic particles.^[12] They undergo a distinct increase in Young's modulus with the application of an external magnetic field.^[13] When subjected to inhomogeneous magnetic fields, magneto-deformation may be experienced making them suitable for the development of small actuators^[14] and even complete devices.^[15] Though the main contribution to actuation lies in magnetodeformation in a nonlinear magnetic field,^[16] slight magnetostriction has also been observed in homogeneous magnetic fields.^[17]

The most common matrix materials are silicones, particularly poly(dimethylsiloxane) or PDMS, though occasionally polyurethane has also been used.^[18] Carbonyl iron is the most commonly used soft magnetic filler material, though hard magnetic materials such as NdFeB have also been employed.^[19] Due to conventional fabrication techniques, the magnetic particle distribution is almost always isotropic though perfect homogeneity is difficult to achieve. In addition, surface structuring techniques are established and well known.^[20]

This work concentrates on the 3D shape memory effects of a hybrid combination of some of the above-mentioned phenomena in the form of magnetic boron–organo–silicon oxide shape memory materials, whose mechanical^[21] and electrical^[22] properties have been recently investigated.

2. Boron–Organo–Silicon Oxide Polymers

Nonlinear viscoelastic-plastic characteristics, such as rheopecty, are typical for many organo–silicon oxide polymers.

Two patents, originally filed during the 1940s^[23,24], first mention the combination of dimethylsiloxane and boric acid for such purposes. The original compound comprised 65% dimethylsiloxane (hydroxy-terminated polymers with boric acid), 17% silica (crystalline quartz), 9% Thixotrol ST (castor oil derivative), 4% polydimethylsiloxane, 1% decamethyl cyclopentasiloxane, 1% glycerine, and 1% titanium dioxide^[25] and the majority of modern compounds deviate little from this. The material is also marketed as a toy under the name “Silly putty” or “bouncing putty.” Industrial uses include deburring and polishing and for rehabilitation therapy in healthcare.

Silicones are widely used, mainly as fluids, emulsions, lubricants, resins, and elastomers. The elastic behavior of silicones is based on the wide-meshed cross-linking of the alternating silicon–oxygen polymer chain backbone. Cross-linking prevents the polymer chains from sliding apart, as is the case with liquids.



The initial hydrolysis reaction exothermically generates a silanol $\text{Si}(\text{CH}_3)_2(\text{OH})_2$ which readily condenses through loss of water to form the siloxane polymer. Since dichlorodimethylsilane is bifunctional (has two chlorines), the chain is able to propagate in two directions generating high molecular weight polymers which retain some residual hydroxyl groups. These residual hydroxyl groups react with boric acid $\text{B}(\text{OH})_3$ to form Si–O–B linkages between polysiloxane chains. Since boric acid is trifunctional, single boron is able to cross-link three polysiloxane chains together. Cross-linking produces a high molecular weight polymer in the form of a soft, pliable gum with very interesting chemical properties.

Sometimes referred to as a “solid-liquid,”^[26] rheologically such materials are dilatant, behaving elastically at high impact rates but flowing like an extremely viscous fluid in the absence of high dynamic force. An additional important attribute concerns temperature dependence. Goertz and coworkers measured the thermal glass transition temperatures for storage modulus and viscosity at angular frequencies up to 100 rad s^{-1} .^[26] What is interesting, from a thermomechanical point, is that the storage modulus changes by two orders of magnitude between 60°C and 100°C whereas a reduction from 60° to -20°C has much less effect.

Such viscoelastic substances flow easily with little applied force. However, with rapidly rising deformation rate, the material hardens and resists flow. This is an extremely important factor where form withdrawal in molding is concerned. Three such models in parallel are used by Goertz^[26] and Hartmann,^[27] while Cross employs the extended Maxwell model^[28] as depicted in **Figure 1** with the inclusion of k_2 .

From Equation (2) the damping factor of the Maxwell function depicted in Figure 1 (without the influence of the second spring constant k_2) can be seen to be highly dependent on velocity. This is the basic characteristics of rheopectic (inverse thixotropic) materials.

$$F = k(l_f - l_{f0}) = C \frac{dl_d}{dt} \quad (2)$$

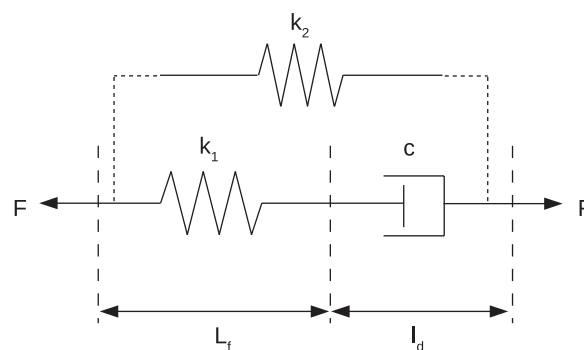


Figure 1. Maxwell model of rheopecty with extended Maxwell (with k_2).

This latter is more appropriate to modeling dynamic behavior and such measurements reveal a clear phase difference between stress and strain resulting in storage and loss moduli. The extended Maxwell model is often employed for illustrating magnetoactive polymers,^[29] though Simulation-X modeling suggesting a four parameter model may be more appropriate.^[30]

3. Magnetoactive Boron–Organo–Silicon Oxide Polymers

The combination of boron–organo–silicon oxide materials with soft ferromagnetic particles has been commercially available for some time.^[31] The use of microparticles ($3.5 \mu\text{m}$ diameter) to form a magnetorheological variant was first investigated by Guo and researchers and a complete characterization including strain rate, creep, relaxation, and dynamic storage modulus has been well documented.^[21] Similar nonrheopectic variations include low molecular weight polyurethane which contain a toluene diisocyanate and polypropylene glycol plastomer, for which a relative magnetorheological effect of over 500% at a flux density of 300 mT is claimed.^[32]

Most researchers have evaluated such viscoelastic materials in oscillatory shear test (OST) mode as if they were fluids, in a rotational rheometer.^[21] However, for shape-memory purposes compressive stress and indentation tests are more relevant. Nano- and microhardness tests (MHT) are also not helpful as they relate only to localized parameters and are more relevant to thin films and coatings.^[33] Uniaxial compression tests (UCT) are more appropriate to large displacements in isotropic materials.^[34]

Poisson's ratio is the ratio of lateral strain to axial strain under uniaxial stress which, in an elastic solid, is related to elastic constants. For viscoelastic materials, Poisson's ratio is not a constant but a time-dependent parameter^[35] and organo–silicon oxide polymers have considerable time dependency. Magnetoactive boron–organo–silicon oxide materials resemble soft clay. Soft clays have Poisson's ratios between 0.4 and 0.5 depending on the level of saturation.^[36] Incompressible fluids have Poisson's ratio of 0.5. The particulate dimensions of clay are similar (between 2 and $6 \mu\text{m}$ diameter) to those of the CIP used in this research (3.5 – $5 \mu\text{m}$).

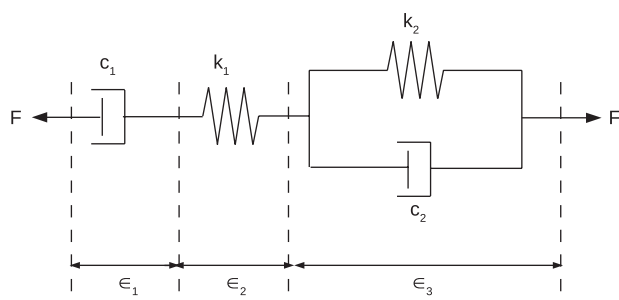


Figure 2. Four parameter Burgers model.

Magnetoactive boron–organo–silicon oxide polymers can best be described by a series combination of Maxwell viscous fluid and Kelvin–Voigt elastic solid. The Maxwell part represents viscous flow in the form of a rising linear characteristic while the Kelvin–Voigt section defines the elastic part given by an exponential rise time which eventually reaches a steady state^[35]. This leads to the Burgers model shown in Figure 2.^[37] The time constants for the Maxwell (rheopexy) and Kelvin–Voigt (creep strain) sections are given by Equations (3) and (4), respectively.

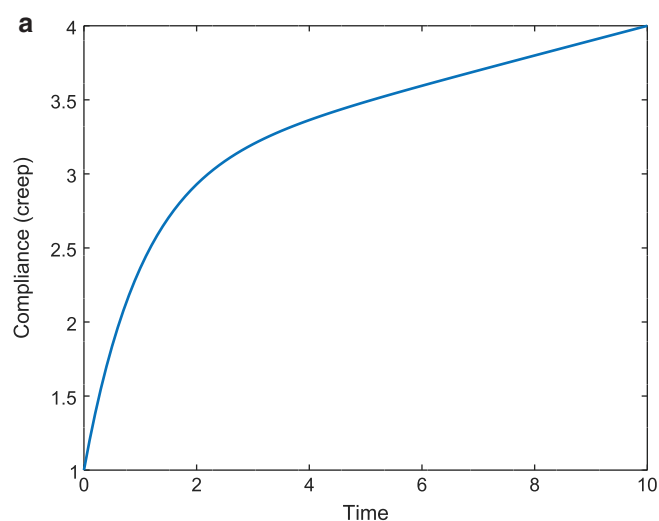
The time constants given in (3) and (4) for each part of the Burgers model are functions of spring constant k [N m^{-1}] and the damping coefficient c [N s m^{-1}].

$$\tau_m = \frac{c_1}{k_1} \quad (3)$$

$$\tau_k = \frac{c_2}{k_2} \quad (4)$$

For an applied stress σ , the total strain is given by Equation (5)

$$\epsilon = \epsilon_1 + \epsilon_2 + \epsilon_3 \quad (5)$$



Creep strain is given by Equation (6) and illustrated in Figure 3a.

$$s(t) = \frac{1}{k_1} + \frac{t}{c_1} + \frac{1}{k_2} \left(1 - e^{-\frac{k_2 t}{c_2}} \right) \quad (6)$$

where s is compliance [$\text{m}^2 \text{N}^{-1}$] given by Equation (7)

$$s(t) = \frac{\epsilon(t)}{\sigma(t)} \quad (7)$$

The spring constant k_1 merely provides an instantaneous strain offset whereas k_2 contributes to delayed elasticity. The damping factor c_1 dictates the steady state while c_2 determines how fast it is reached. For a magnetic hybrid, the applied magnetic field has a significant influence on c_1 .

Calculation of (7) can easily be achieved using any computer system (e.g., MatLab or BASIC). See Supporting Information for examples. For normal viscoelastic materials, example parameters: $k_1 = 1$, $k_2 = 0.5$, $c_1 = 10$, $c_2 = 0.5$ give exponentially increasing creep (arbitrary units) which tends to a steady state for a given time as shown in Figure 3a. For normal boron–organo–silicon oxide polymers (without magnetic fillers) all these values are much larger. Cross^[28] uses $k_1 = 8000$, $k_2 = 380$, $c_1 = c_2 = 89\,000$ which results in a straight line, i.e., constant creep rate. However, for the purposes of magnetic shape memory, the relaxation characteristics are more important.

The rate at which the compliance changes is given by differentiating Equation (6) with respect to time (8).

$$\frac{\partial s}{\partial t} = \frac{1}{c_1} + \frac{1}{c_2} e^{-\frac{k_2 t}{c_2}} \quad (8)$$

As in solid mechanics where compliance is the reciprocal of elastic modulus, for a viscous fluid compliance has the same

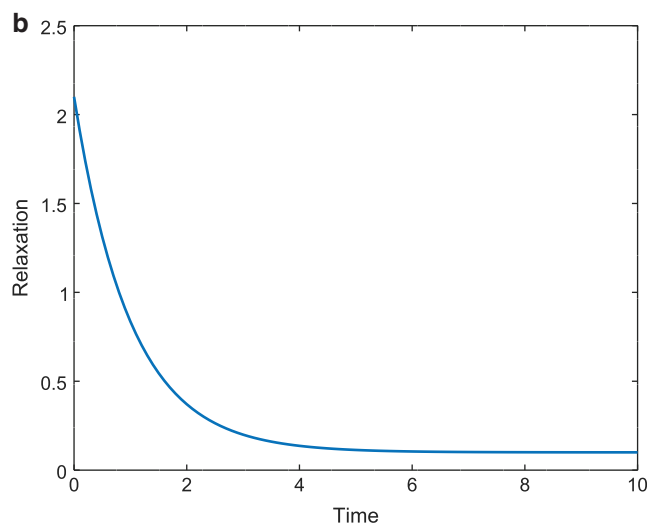


Figure 3. a) Compliance and b) relaxation as functions of time.

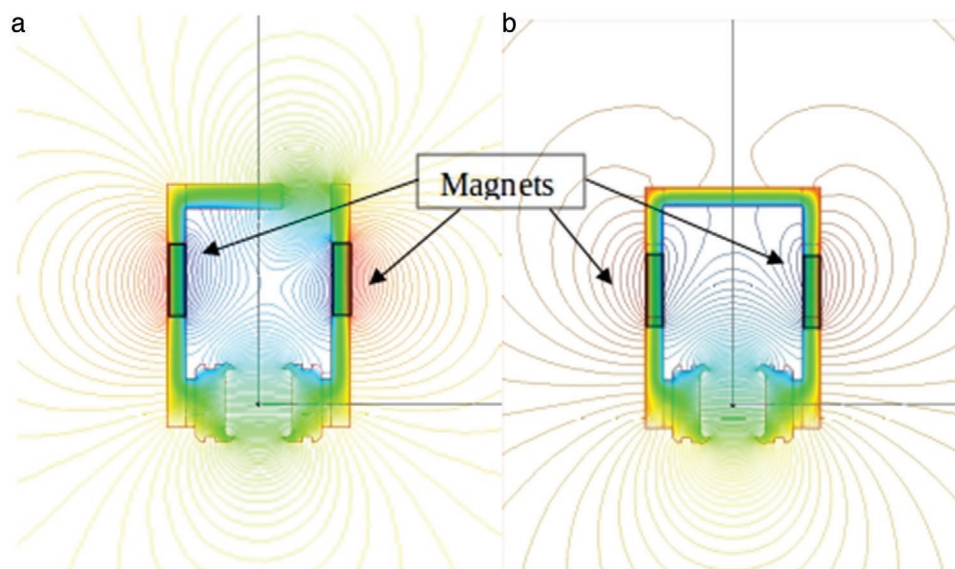


Figure 4. Magnetic field homogeneity: a) improved and b) original.

units. The rate of change of compliance (8) has units $[m\ s\ kg^{-1}]$ with is the reciprocal of viscosity. Using the same example parameters with Equation (8) reveals an exponentially reducing relaxation against time as illustrated in Figure 3b.

In the case of magnetoactive boron–organo–silicon oxide polymers under the influence of a magnetic field, the viscous contribution is much lower. In fact, for low strain rates, such materials are basically plastic and more akin to sandy soft clay than conventional polymers or rubber. As a result, k_1 remains almost constant while parameters c_1 and c_2 are reduced. However, k_2 is significantly increased which results in the long steady state condition important to magnetic shape memory effects.

Furthermore, being rheopectic, boron–organo–silicon oxide polymers demonstrate elasticity only when subjected to very high stress rates. Although irrelevant to the shape memory effect itself, this attribute is significant in demolding operations.

The storage modulus increases with CIP content and magnetic flux density but tends to reach saturation at around 0.5 T. The application of a magnetic field restricts creep^[21] which makes such hybrid materials suitable for volumetric shape memory applications. Contrary to magnetoactive elastomers, magnetoactive boron–organo–silicon oxide materials are viscoelastic and so do not immediately return to their original state on removal of the magnetic field. This results in long shape retention lifetimes. In the absence of a magnetic field, room temperature thermal excitation is adequate for resetting the material to its quiescent state over time. This can be expedited by raising the temperature, for which there are many possible methods. The resetting of superparamagnetic nanoparticle doped SMP has been demonstrated by means of radio frequency (300 kHz) induction heating. However, power densities in the range of $30W\ g^{-1}$ are required to reach the glass transition temperature.^[38] Alternatives for conventional magnetoactive polymers include infrared and microwaves.^[15]

4. Experimental Section

Traditional PDMS based magnetoactive elastomers may be made soft and pliable^[20] and have been used for 3D shape memory functions.^[39] However, the inherent elasticity of the magnetoactive polymer limits the impression depth. Magnetoactive organo–silicon oxide polymers are soft viscoelastic materials which have very long relaxation times thus giving the impression of temporary plasticity.

Commercially available boron–organo–silicon oxide polymers (www.knete.de) were combined with 50wt% carbonyl iron powder (CIP) particles with a diameter range 3.9–5.0 μm (BASF SQ) by mechanically kneading at a temperature of 37 °C. Generally, the higher the CIP concentration, the better the shape memory effect. However, due particle agglomeration, over 60wt% CIP is difficult to mix completely by kneading. In order to prolong the shape memory effect, the magnetoactive boron–organo–silicon oxide polymer samples must be maintained within a homogeneous magnetic field. This can be achieved by appropriate choice of pole shoes and magnetic field circuit as shown in Figure 4.

In conventional devices used to vary magnetic fields, a second air gap can be inserted at one side in order to increase the magnetic resistance in the yoke.^[40] As can be seen in Figure 4, this improves magnetic field homogeneity at the price of slightly reduced magnetic field strength. The use of permanent magnets eliminates any interference from stray fields resulting from electromagnetic induction where current driven magnetic field sources are employed. The homogeneity of the magnetic field was verified by means of a Gaussmeter (Lakeshore 455 DSP) mounted on a 6 axis Stäubli RX60^[41] precision industrial robot. The magnetic field flux density could be adjusted by changing the distance of the permanent magnets along the yoke. With pole shoes of 40 mm diameter, a magnetic field with good homogeneity is possible for a volume of at least 1 cm^3 . Figure 5 demonstrates this with a magnified view of the flux lines between the pole shoes.

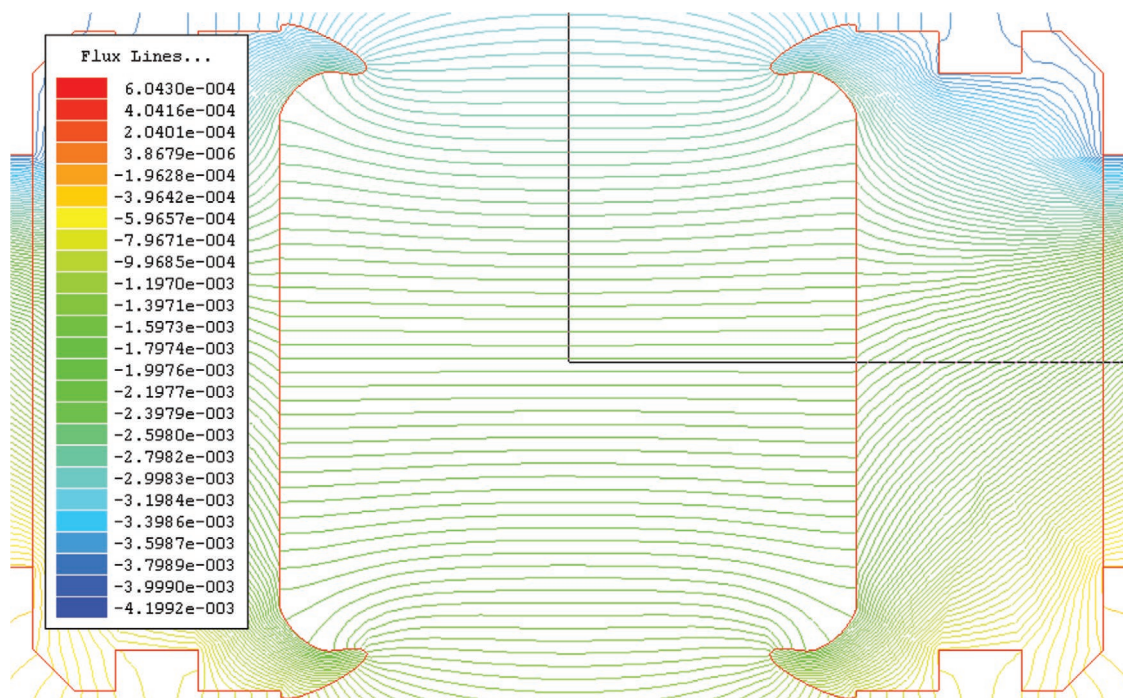


Figure 5. Detailed view of homogeneous magnetic field volume.

For the purposes of this work, the magnetic flux density (sample in situ) was adjusted to 22 mT in the center. Within a 3 cm cubic volume between the pole shoes, the deviation was less than 1 mT. The magnetic field strength is not so critical but too high a flux density and the mold tends to be pulled toward the magnetic field, too little and the relaxation time constant (τ) is reduced.

Two samples were produced from identical impressions of a small LEGO™ brick, pressed into the material to a depth

of 5 mm. An indentation depth of 5 mm was chosen because this corresponds to exactly half the homogeneous magnetic field volume. One was placed within the homogeneous magnetic field, depicted in Figure 5, the other without magnetic flux. Both were left for several hours at room temperature (23 °C) and normal atmospheric pressure. Figures 6a and 7a show the effectively identical imprints with and without an applied magnetic field, directly after impression. A slight difference is observable between Figures 6b and 7b even after

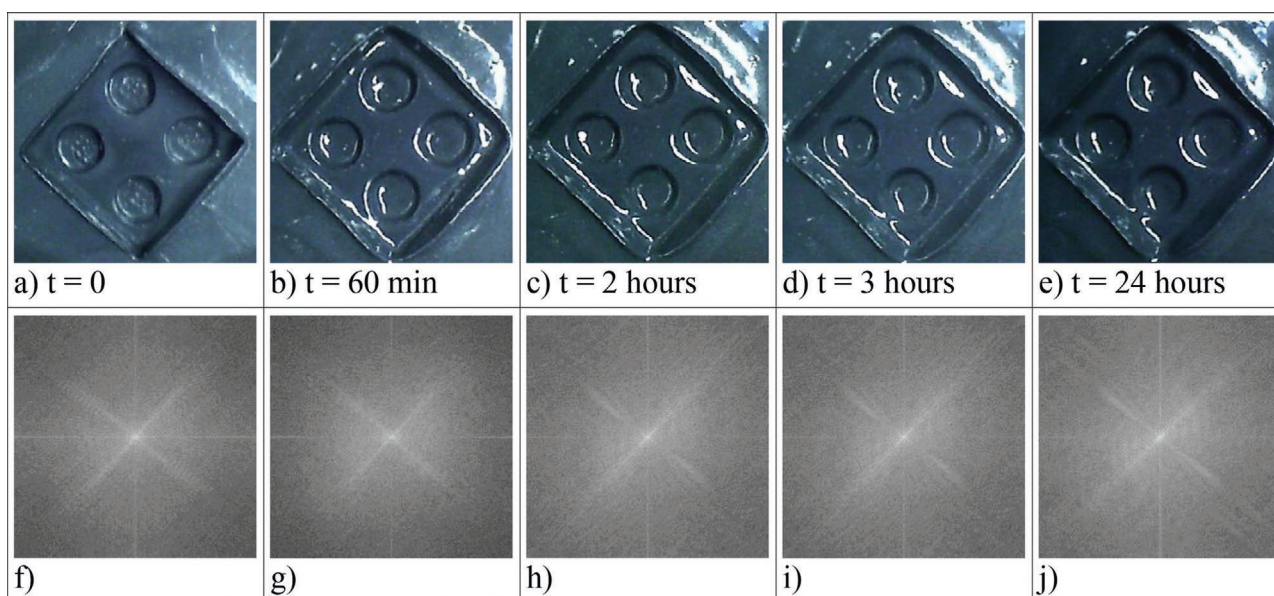


Figure 6. Images of samples subjected to magnetic field (a–e) and their Fourier transforms (f–j).

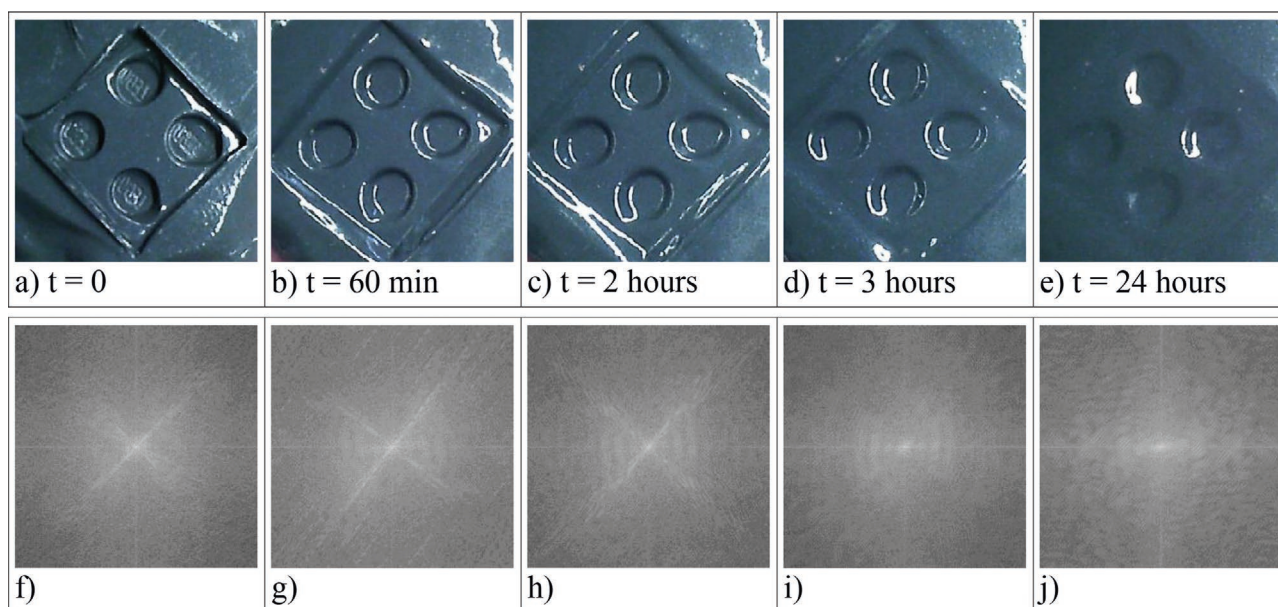


Figure 7. Images of sample in absence of magnetic field (a–e) and their Fourier transforms (f–j).

60 min with and without magnetic field, respectively. After 120 min, a clear smoothing of the image without the magnetic field can be seen in Figure 7c, where the indentation after 2 h has reduced to below 2 mm, compared to that of Figure 6c where the 5 mm indentation depth remains. A similar progression can be observed after 3 h and after 24 h the imprint is still discernible with the magnetic field whereas that without a magnetic field, shown in Figure 7e, has almost completely disappeared.

A Fourier transform is effectively the portrayal of the features of a two dimensional image in the frequency domain.^[42] The center represents the lowest frequencies while those further from the center pertain to higher frequencies, i.e., fine detail. The vertical and horizontal components of the Fourier transform are largely a result of the vertical and horizontal borders, respectively. Thus the deliberate 45° rotation of the images results in Fourier components, pertaining to image details in the diagonal. This becomes very clear in Figure 7j.

In all the Fourier transforms in Figure 6, the strong Fourier components pertaining to the image features are maintained even for as long as 24 h. In Figure 7, the loss of the high frequencies commences almost immediately in absence of a magnetic field. Severe smoothing appears after 2 h and after 3 h the Fourier transform shows little meaningful detail. After 24 h, the image is a mere shadow of the original imprint and the remaining vertical and horizontal lines result from the borders of the image while those pertaining to the actual features have disappeared completely.

5. Applications

There are numerous potential applications for magnetoactive boron–organo–silicon oxide polymers, many of which

are described in more detail in the references. This work concentrates on static shape memory applications, two of which will be briefly discussed here.

5.1. Rapid Prototyping

For prototypes, 3D printing can be time consuming (generation of a CAD model, printing and rework). For large batch sizes, conventional injection molding is more appropriate but comparatively expensive. Temporary wax molding may be more cost effective for small batches but the wax must be melted before being reformed and left to cool prior to reuse. Magnetoactive organo–silicon oxide polymers have the advantage of rapid mechanical forming without energy intensive thermal operations. Under the influence of an applied magnetic field, the material remains rigid for the duration of the molding process. On completion, removal of the magnetic field allows immediate reuse. Unnecessary energy consumption can be avoided through the employment of permanent magnets rather than electromagnets. Materials such as plaster, epoxy resin, and RTV rubbers can be easily molded.

As noted by Goertz,^[26] the effects of temperature on the viscosity of organo–silicon oxide can be significant, particularly at temperatures over 50 °C. However, with magnetoactive boron–organo–silicon oxide the effects are not so dramatic. As measured by Guo, the storage modulus is merely halved with a five-fold temperature increase.^[21] In fact, even thermoplastic materials with relatively high melting temperatures (measured as 56.4 °C using a FLIR TG167 infra-red camera) have been easily molded without damage to or distortion of the boron–organo–silicon oxide mold.

One of the greatest problems associated with molding technology lies in the removal of the form without distortion of the mold. As explained previously, boron–organo–silicon oxide

polymers are rheopectic. This means extraction and demolding can be achieved through rapid and abrupt withdrawal, rather than futile attempts to slowly and carefully dislodge the form from the mold as is the case with conventional putty or magnetoactive elastomeric materials.^[43]

5.2. Robotic Prehension

Conformable surfaces for the purposes of automated prehension of geometrically irregular components have constituted an area of investigation in robotics for many years. Omnigrippers comprising displaceable metal pegs,^[44] powder filled bags,^[45] shape memory foams,^[46] magnetorheological fluids,^[47] and magnetoactive polymers^[48] to name but a few examples. With all such designs there exist two major problems. The degree of compliance may be limited and where thermal techniques are employed, a continuous flow of energy may be required. As mentioned above, where a magnetic field is required, permanent magnets can provide a very low energy solution.

Magnetoactive boron–organo–silicon oxide polymers provide theoretically unlimited compliance while fulfilling the necessary requirements of low energy object retention. Unlike magnetorheological fluids, magnetoactive boron–organo–silicon oxide polymers are plastically deformable solids so there is no danger of leakage and contamination.

6. Conclusions

The long-term static characteristics of boron–magnetoactive organo–silicon oxide polymers have been evaluated with regard to their relevance to three-dimensional shape memory applications, for which they have been demonstrated to be considerably superior to conventional magnetoactive materials. By means of Fourier transforms, the degradation of fine detail over time has been analyzed and samples with and without magnetic field influence compared.

The ability of magnetoactive boron–organo–silicon oxide polymers to retain topological profiles for long periods makes a significant contribution to reconfigurable molding in rapid prototyping and conformal surfaces generally. Obviation of the necessity for continuous energy supply is a further advantage over thermal shape memory methods. The extension to robotic prehension and similar shape memory applications stands to reason.

Supporting Information

Supporting Information is available from the Wiley Online Library or from the author.

Acknowledgements

The authors would like to express their gratitude to the Deutsche Forschungsgemeinschaft (DFG) for financial support within the SPPI681 (MO 2196/2-1). Open access funding enabled and organized by Projekt DEAL.

Conflict of Interest

The authors declare no conflict of interest.

Keywords

boron–magnetoactive organo–silicon oxide polymers, magnetoactive elastomers, volumetric shape memory effect

Received: April 25, 2020
Revised: June 6, 2020
Published online: July 8, 2020

- [1] A. Martens, *VDI Zeitschrift* **1878**, 22, 11.
- [2] H. Czichos, in *The Martensitic Transformation in Science and Technology* (Eds. E. Hornbogen, N. Jost), Informationsgesellschaft, Oberursel, Germany **1989**, pp. 3–14.
- [3] E. Hornbogen, *Adv. Eng. Mater.* **2006**, 8, 1.
- [4] D. E. Hodgson, M. H. Wu, R. J. Biermann, *Properties and Selection: Nonferrous Alloys and Special-Purpose. ASM Handbook*, Vol. 2, ASM International, Materials Park, OH **1990**, pp. 897–902.
- [5] B. K. Kim, S. Y. Lee, M. Xu, *Polymer* **1996**, 37, 5781.
- [6] P. T. Mather, X. Luo, I. A. Rousseau, *Annu. Rev. Mater. Res.* **2009**, 39, 445.
- [7] Q. Zhao, H. J. Qi, T. Xie, *Prog. Polym. Sci.* **2015**, 49–50, 79.
- [8] G. J. Monkman, *Ind. Robot* **1991**, 18, 31.
- [9] K. Gall, M. Mikulas, N. A. Munshi, F. Beavers, *J. Intell. Mater. Syst. Struct.* **2000**, 11, 877.
- [10] H. Meng, G. Li, *Polymer* **2013**, 54, 2199.
- [11] F. Pilate, A. Toncheva, P. Dubois, J. -M. Raquez, *Eur. Polym. J.* **2016**, 80, 268.
- [12] A. Dorfmann, R. W. Ogden, *Eur. J. Mech.* **2003**, 22, 497.
- [13] A. Stoll, M. Mayer, G. J. Monkman, M. Shamonin, *J. Appl. Polym. Sci.* **2014**, 131, 39793.
- [14] D.-G. Hwang, M. D. Bartlett, *Nat. Sci. Rep.* **2018**, 8, 3378.
- [15] K. Zimmermann, V. Böhm, T. I. Becker, J. Chavez Vega, T. Kaufhold, G. J. Monkman, D. Sindersberger, A. Diermeier, N. Prem, *Int. Sci. J. Probl. Mech.* **2017**, 4, 1512.
- [16] P. Von Lockette, R. Sheridan, at Proc. of the ASME 2013 Conf. on Smart Materials, Adaptive Structures and Intelligent Systems, Snowbird, UT, USA, September **2013**.
- [17] V. Sorokin, G. Stepanov, M. Shamonin, G. J. Monkman, A. R. Khokhlov, E. Y. Kramarenko, *Polymer* **2015**, 76, 191.
- [18] K. Petcharoen, A. Sirivat, *Mater. Sci. Eng., C* **2016**, 61, 312.
- [19] H. Böse, A. Hesler, G. Monkman, *Deutsche Patent DE 10 2007 028 663 A1*. Priority: 21.06.2007. *European Patent EP 2 160 741 B1 Granted: 17.08. 2011*.
- [20] E. Forster, M. Mayer, R. Rabindranath, H. Böse, G. Schlunck, G. J. Monkman, M. Shamonin, *J. Appl. Polym. Sci.* **2013**, 128, 2508.
- [21] F. Guo, C. Du, G. Yu, R. Li, *Adv. Mater. Sci. Eng.* **2016**, 2016, 1.
- [22] G. J. Monkman, B. Striegl, N. Prem, D. Sindersberger, *Macromol. Chem. Phys.* **2020**, 221, 1900342.
- [23] R. R. McGregor, E. L. Warrick, *US Patent No. 2,431,878*, **1947**.
- [24] J. G. E. Wright, *US Patent No. 2,541,851*, **1951**.
- [25] T. Ikematu, Y. Kishimoto, K. Miyamoto, *US Patent 5,189,110*, **1993**.
- [26] M. P. Goertz, X. -Y. Zhu, J. E. Houston, *J. Polym. Sci.: B: Polym. Phys.* **2009**, 47, 1285.
- [27] L. Hartmann, R. Reich, U. Kletzin, L. Zentner, *58th Ilmenau Scientific Colloquium*, Technische Universität Ilmenau, Ilmenau **2014**.
- [28] R. Cross, *Am. J. Phys.* **2012**, 80, 870.
- [29] T. A. Nadzharyan, V. V. Sorokin, G. V. Stepanov, A. N. Bogolyubov, E. Yu. Kramarenko, *Polymer* **2016**, 92, 179.



- [30] P. Kugler, *Simulation X: Simulation magnetoaktiver Polymere*, OTH-Regensburg, Bachelorarbeit **2015**.
- [31] Crayola LLC – 2025 Edgewood Ave, Easton, PA 18040, USA.
- [32] Y. Xu, X. Gong, S. Xuan, W. Zhang, Y. Fan, *Soft Matter* **2011**, *7*, 5246.
- [33] Z. Chen, S. Diebels, *Technische Mechanik* **2014**, *34*, 166.
- [34] International Standard ISO 604:2002(E): *Plastics – Determination of Compressive Properties*, 3rd edition, ISO **2002**.
- [35] W. N. Findley, J. S. Lai, K. Onaran, *Creep and Relaxation of Nonlinear Viscoelastic Materials*, North-Holland Publishing, New York **1976**.
- [36] D. E. Newcomb, B. Birgisson, *Measuring in Situ Mechanical Properties of Pavement Subgrade Soils*, National Academy Press, Washington **1999**.
- [37] A. Y. Malkin., A. I. Isayev, *Rheology: Concepts, Methods, and Applications*, ChemTec Publishing, Toronto **2006**.
- [38] A. M. Schmidt, *Macromol. Rapid Commun.* **2006**, *27*, 1168.
- [39] L. V. Nikitin, G. V. Stepanov, L. S. Mironova, A. I. Gorbunov, *J. Magn. Magn. Mater.* **2004**, *272-276*, 2072.
- [40] C. Yamanaka, M. Ikea, K. Meguro, A. Nakanishi, *Int. J. Radiat. Appl. Instrum. D. Nucl. Tracks Radiat. Meas.* **1991**, *18*, 279.
- [41] Stäubli, RX60 Robot, CS7M controller, D.280.059.04.F – 11/1999.
- [42] F. Van der Heijden, *Image-based Measurement Systems*, John Wiley, Chichester **1994**.
- [43] P. Testa, R. W. Style, J. Cui, C. Donnelly, E. Borisova, P. M. Derlet, E. R. Dufresne, L. J. Heyderman, *Adv. Mater.* **2019**, *31*, 1970207.
- [44] P. B. Scott, *Robotica* **1985**, *3*, 153.
- [45] T. Reinmüller, H. Wiessmantel, *Proc. Int. Symp. on Industrial Robots*, IFS Publications, Springer Verlag, Berlin **1988**, p. 241.
- [46] G. J. Monkman, *Mechatronics* **2000**, *10*, 489.
- [47] A. Pettersson, S. Davis, J. O. Gray, T. J. Dodd, T. Ohlsson, *J. Food Eng.* **2010**, *98*, 332.
- [48] K. Zimmermann, J. Chavez Vega, T. Becker, H. Witte, C. Schilling, S. Köhring, V. Böhm, G. J. Monkman, N. Prem, D. Sindersberger, I. Lutz, *Probl. Mechanics.* **2019**, *2*, 23.